Manuscript submitted to
AIMS' Journals
Volume **X**, Number **0X**, XX **200X**

Website: http://AIMsciences.org

pp. **X–XX**

MODELING GROUP DYNAMICS OF PHOTOTAXIS: FROM PARTICLE SYSTEMS TO PDES

Doron Levy

Department of Mathematics
and
Center for Scientific Computation and Mathematical Modeling (CSCAMM)
University of Maryland
College Park, MD 20742, USA

Tiago Requeijo

Department of Mathematics
Stanford University
Stanford, CA 94305-2125, USA

(Communicated by Aim Sciences)

Abstract. This work presents a hierarchy of mathematical models for describing the motion of phototaxis, i.e., bacteria that move towards light. Based on experimental observations, we conjecture that the motion of the colony towards light depends on certain group dynamics. This group dynamics is assumed to be encoded as an individual property of each bacterium, which we refer to as 'excitation'. The excitation of each individual bacterium changes based on the excitation of the neighboring bacteria. Under these assumptions, we derive a stochastic model for describing the evolution in time of the location of bacteria, the excitation of individual bacteria, and a surface memory effect. A discretization of this model results in an interacting stochastic many-particle system. The third, and last model is a system of partial differential equations that is obtained as the continuum limit of the stochastic particle system. The main theoretical results establish the validity of the new system of PDEs as the limit dynamics of the multi-particle system.

1. **Introduction.** Bacteria live in environments that can be often limiting for growth. As a result, they have evolved sophisticated mechanisms in order to sense changes in environmental parameters such as light and nutrients. Under certain conditions, such changes will initiate a motion of an individual bacteria (or even of an entire colony) in order to increase the resources availability.

In this work we are interested in the motion of Cyanobacteria, that are a lineage of ancient, ubiquitous photosynthetic microbes. Cyanobacteria track light direction and quality to optimize conditions for photosynthesis. The motility toward a light source is called "phototaxis" and requires a photoreceptor, a signal transduction event, and a motility apparatus. In a series of experiments reported in [7], time-lapse video microscopy was used to monitor the movement of individual cells and groups of cells. These movies suggest that in addition to the ability of single cells

2000 *Mathematics Subject Classification.* Primary: 92C17; Secondary: 92C80, 82C22, 65C35.
Key words and phrases. Phototaxis, Chemotaxis, Group Dynamics, Stochastic Particle Systems.

to move directionally, the overall time-evolution is determined by means of a group dynamics. For example, even when a directional light is continuously present, it takes a significant time for the cells to initiate a motion towards light. It is also observed that individual cells are less likely to move towards light while while cells that are grouped together are more likely to move. Some surface memory effects are also observed, i.e., it seems to be easier for bacteria to travel on surfaces that were previously visited by other bacteria. Overall, the various patterns of movement that we observe appear to be a complex function of cell density, surface properties and genotype. Almost nothing is known about the nature of the interactions between these parameters for Cyanobacteria.

In this work we derive several mathematical models for the motion of phototaxis that take into account certain assumptions about the nature of the group dynamics. More specifically, we assume that every bacteria has an internal property, which we refer to as its 'excitation'. The excitation of any bacterium is a time-dependent quantity that is adjusted based on the excitation of the neighboring bacteria. The excitation of a bacteria must exceed a pre-determined threshold for it to initiate a motion in the direction of light.

In that spirit, our first model is a stochastic model in which we track in time the locations of the individual bacteria, their excitation, and their trajectories in space. Numerical simulations of this stochastic model show a qualitative behavior that is similar to the observed experimental data.

Our second model is a stochastic particle model that is obtained from a discretization of Model I. In this model all three quantities (bacteria, excitation, and surface) are converted into particles. Rules of motion as well as birth/death rules for all particles determine their dynamics. In particular, excitation particles are assumed to move together with their associated bacteria, but since excitation for any individual bacterium can change in time, excitation particles are allowed to give birth and die. Finally, our last model, is a continuous model that is written as a system of PDEs for the evolution of the densities of bacteria, excitation, and the surface memory effect. Most of this paper deals establishing the limit of the particle system as the system of PDEs. The techniques we use follow the works of Oelschläger [14] for reaction-diffusion equations, and of Stevens [18] for chemotaxis. When compared with the work of Stevens, the inclusion of the "excitation" property, does require us to make some additional assumptions and to adjust some of the estimates.

Over the past several decades, there has been a lot of activity in the mathematical community in studying mathematical models for chemotaxis (i.e. bacteria that move in the direction of a chemical attractant), starting the pioneering work of Patlack [16], and the similar Keller and Segel model [12]. Most of the recent research efforts concentrate on studying finite-time blowup for the Keller-Segel model or preventing such a blowup using various regularizations. Since at this point, these studies have very little connection to the focus of our present work, we do not provide a list of references. We rather refer the interested reader to the recent work of Hillen, Painter, and Schmeiser, that contains a comprehensive overview of the state-of-the-art studies of the Patlack-Keller-Segel model [11].

In spite the interest of the mathematical community in chemotaxis, phototaxis models are almost nowhere to be found. Few examples include [19] and [21], none of which considers the group dynamics as a mechanism that is important to the motion. This paper is the first attempt in that direction. Finally, we note that

(a) 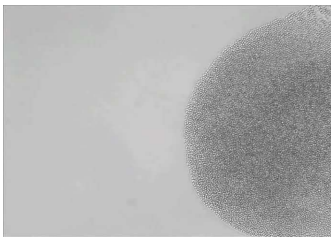 (b) 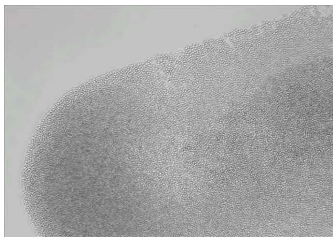

FIGURE 1. Bacteria motion when the density is high. The snapshots were taken at increasing times. The light comes from the left of the domain.

we have introduced the stochastic model and its simulations in a recent conference proceedings [4]. An extensive simulation study of the stochastic model is currently in progress and is left for a future publication. For completeness we do include in this paper examples of the numerical simulations that can be obtained using the stochastic model.

The structure of this paper is as follows: Our first model, the stochastic model, is introduced in Section 2. The presentation starts with a summary of experimental observations, proceeds with the mathematical framework, and concludes with numerical simulations. The other two models, the many-particle system, and the limit system of PDEs are introduced in Section 3. We start with the particle system in Section 3.1. The densities that will be used in the continuous description are defined in Section 3.2. The dynamics of the particles that is described in Section 3.3. The formal derivation of the limit dynamics as a system of PDEs is carried out in Section 3.4. The limit theorems that establish that limit are given in Section 3.5. Section 4 is devoted to the proof of Theorem 3.2. Concluding remarks are given in Section 5.

2. **A Stochastic Model for Phototaxis.**

2.1. **Experimental Observations.** In [7] Bhaya and Burriesci used time-lapse video microscopy to track the movement of cells. An analysis of these videos has led us to the following observations regarding the characteristics of the motion:

1. *Delayed motion.* Even when the light is on, it will typically take a long amount of time (minutes to hours) for the bacteria to make a decision to start moving towards the light. When such a motion is initiated, it always starts in areas of a high-density of bacteria. Individual bacteria will almost never initiate a motion towards light.
2. *High density motion.* When the density of the cells is high, bacteria tend to move towads the light in one group (see Fig. 1).
3. *Fingering.* In areas of low-density, bacteria tend to remain still, while when the density of bacteria is high, cells tend to move faster. Such a "competition" between the inhomogeneously populated regions results with *fingers* such as those that can be seen in Fig. 2. Bacteria that are end up being on the edges of these fingers stop moving (or move very slowly). In some cases it is even possible to observe a *pinching*. This happens when the density of cells is high enough to form a finger but as the finger is formed and bacteria move towards

(a) 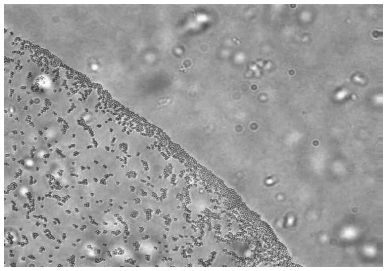 (b) 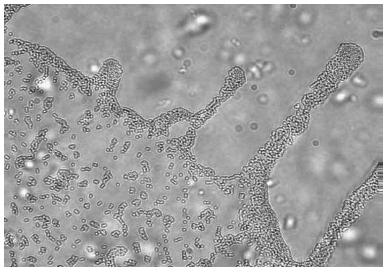

FIGURE 2. Creation of fingers with a light source at the upper-right corner of the domain. Figure (a) shows the edge of the colony with single cells showing as dark dots. Figures (b) taken several hours later show the bacteria moving toward the light source.

(a) 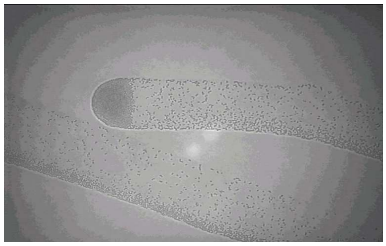 (b) 

FIGURE 3. Bacteria follow a similar pattern of motion on locations that were traveled by other bacteria. Shown are snapshots taken at consecutive times. The light source is from the left.

the light source, the density behind the leading tip decreases. Then, if there are not enough bacteria present, the tip eventually detaches.

4. *A surface memory effect.* The movies suggest that when the cells move, they mark the surface in a way that makes it for other cells more likely to revisit locations that were already traveled by other bacteria. In the time scales we are interested in (hours), our observations indicate that this surface memory effect does not decay at all, or perhaps has a very slow decay rate. Such a memory effect is demonstrated in Fig. 3.

2.2. **The Mathematical Framework.** To derive a model that is based on the observations and assertions above, we need to specify three different stochastic processes. The first two concern the position of each bacterium and its excitation at a specific moment in time, while the third process determines the memory effect of the medium at a specific point in space and time. To that end, we let N denote the number of bacteria present in a free boundary medium ($\mathbb{R}^2$) and denote by $X_i(t) \in \mathbb{R}^2$ the position of bacterium i at time $t \geq 0$.

We start by assuming that the first process, L, which denotes the memory surface effect, is a pure jump process that is given by

$$L(t;x,y) = \max_{\substack{0\leq s\leq t \\ i=1,\ldots,N}} \delta_{(x,y)}(X_i(s)), \tag{1}$$

where $\delta_{(x,y)}$ is the Dirac delta in $\mathbb{R}^2$. While not assuming any particular biological process that is responsible for this memory effect (such as a slime mold), equation (1), simply means that bacteria "mark" the trajectories in $\mathbb{R}^2$ on which they travel.

Remark 1. The experimental evidence indicates that the surface memory effect does not diffuse over time or diffuses very slowly (this is definitely the case for the time frame in which the movies are taken, i.e., several hours). Equation (1) is therefore written without a diffusion term. In the context of Section 3, mainly due to technical reasons, we will add a diffusion term to the stochastic process L. In either case, it can be assumed to be negligible.

Remark 2. It would probably be more realistic to assume the external substance is produced in a continuous manner, rather than by a pure jump process. However, in the setting of the multi-particle system discussed in Section 3, this difference does not play an important role. Also, according to our assumptions, the quantity of such a substance should quickly increase when it is in contact with bacteria (up to a certain level). Hence, even from practical considerations, when simulating the model, the best way to discretize this process is according to (1).

The second process is the "excitation process". We denote the excitation process for particle i by S_i and let $\mu_i(t)$ be a weighted average of the total excitation in a given neighborhood of particle i at time t. An example of such a function $\mu_i(t)$ is

$$\mu_i(t) = \frac{1}{N}\sum_{j=1}^{N}\left[\left(1 - \frac{d(X_j(t), X_i(t))}{2}\right)^+ S_j(t)\right],$$

where $d(\cdot,\cdot)$ is the Euclidean distance between the points, and $(a)^+$ denotes the positive part of a. We will assume that $S_i(t)$ is given by a geometric mean-reverting process

$$\frac{dS_i(t)}{S_i(t)} = (\mu_i(t) - S_i(t))dt + \sigma dW_i(t), \tag{2}$$

where σ is constant (a property of the bacteria) and W_i, $i = 1, \ldots, N$ are independent Brownian motions.

With $\mu_i(t)$ and $S_i(t)$ defined this way we know that $S_i(t) > 0$ for all $t \geq 0$ and also that $S_i(t)$ tends to move towards the mean reverting level $\mu_i(t)$. Hence, controlling $\mu_i(t)$ will implicitly control $S_i(t)$ (in particular, if μ_i is bounded then the same will hold for S_i almost surely).

The third process is the position process, $X_i(t)$. Here, the motion towards light should be taken into account. We thus assume that ξ_t is a unit vector that represents the direction from which bacteria sense the light at time t. Together with the bacteria sensitivity to the surface memory, this can be encoded into a C^∞ function $q\colon \mathbb{R}_0^+ \times \mathbb{R}_0^+ \times \mathbb{R}^2 \to [0,1]$ satisfying

1. q is strictly increasing in the first two variables.
2. $\lim_{s\to\infty} q(s,\cdot,\cdot) = 1$.
3. $q(0,\cdot,\cdot) = 0$.

We can thus define

$$dX_i(t) = v_s q\left((S_i(t) - K)^+, L(t;x,y), \nabla L^N(t;x,y)\right)\xi_t dt + v_r d\tilde{W}_i(t), \tag{3}$$

where $\tilde{W}_i(t)$ are independent 2-dimensional Brownian motions and v_s, v_r are the maximum velocity components for 1) excitation and sensitivity to external substance, 2) the random phenomena. For each $N > 0$, L^N is the stochastic process obtained from L by a convolution with a mollifier. Equation (3) is designed in a way that guarantees that bacteria tend to move in the direction of light only if the excitation exceeds the predetermined threshold K. In such cases, the surface memory effect is also taken into account in the overall motion towards light. If the excitation of an individual bacterium does not pass the threshold K, the only mechanism that controls its motion is a random phenomenon. This model thus accounts for sensitivity to the extra substance, sensitivity to light, and random phenomena.

Remark 3. In order to take into account the possibility of time periods without any light, the processes $S_i(t)$ can be changed by either making them decay fast when the light source is not present or even by making them jump to values below the threshold K at the moment the light source vanishes.

Remark 4. The main difference between our model of phototaxis and the chemotaxis model of Stevens [18] resides in the existence of the *excitation* quantity, which is an internal property of each bacteria. Equation (2) has the desired effect that an individual's excitation will evolve towards a surrounding neighborhood trend (given by $\mu_i(t)$). The excitation serves as a mechanism for taking into account the group dynamics. The threshold that the excitation must pass in order to initiate a motion toward light serves as a way for encoding the observed delay in the response of the bacteria to light.

2.3. **Numerical Simulations.** We used the model described in Section 2.2 to simulate the behavior of this bacteria population. The simulation is done by discretizing (1), (2) and (3) for small time increments. The functions and parameters that were used in our simulations are: $\Delta t = 0.1$, $\sigma = 0.3$, $K = 0.1$, $v_s = 3.0$, $v_r = 0.05$, and $q(s, w, v) = \alpha(w, v)\big(1 - exp(-s)\big)$, where $\alpha(w, v) = \max\{w, v \cdot \xi_t, 0.2\}$. For the sake of brevity, we refer to [5] for the details of the discretizations of the model equations.

In Figures 4, 5, 6 we show snapshots at different times of a bacteria motion in the direction of a light source that is located to the left of the domain. Bacteria surrounded by a higher number of individuals tend to move faster.

Under certain conditions, one can localize the bacteria to a point that there is a seemingly unlimited growth in their density. One possible mechanism to obtain such a result is to change the direction of the light source in time in a way that collapses all the particles into a small area. This is the result of a higher percentage of surface being marked, as well as an uniformly high density of particles. In this way, particles are allowed to move faster, and thus concentrating on small areas. Such an example is shown in Figure 7. In this simulation we start with 5000 bacteria that are normally distributed in $\mathbb{R}^2$. The light changes its direction according to the iterations indicated in Table 1. Figure 7 shows the snapshots taken at iterations 100, 140, 230, and 360.

In some experiments it was observed that the tip of a finger can separate from the rest of the finger. This "pinching" phenomenon as obtained in our numerical simulations, is demonstrated in Figure 8. This sequence shows the tip detaching, shortly after a finger is formed. This effect is a result of a mixture of areas of lower and higher density of particles. Although the finger is formed due to a high density of particles, there are not enough particles on the back of the domain to keep up with the forming tip, leading to its detachment.

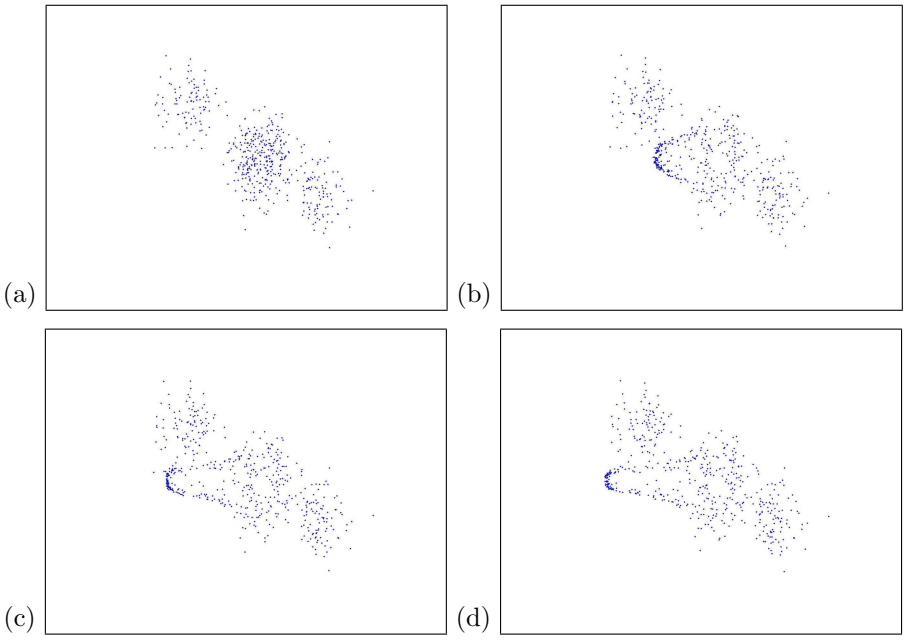

FIGURE 4. A simulation of a bacteria motion towards the light source, on the left. The initial distribution has one area with high density and one area with low density.

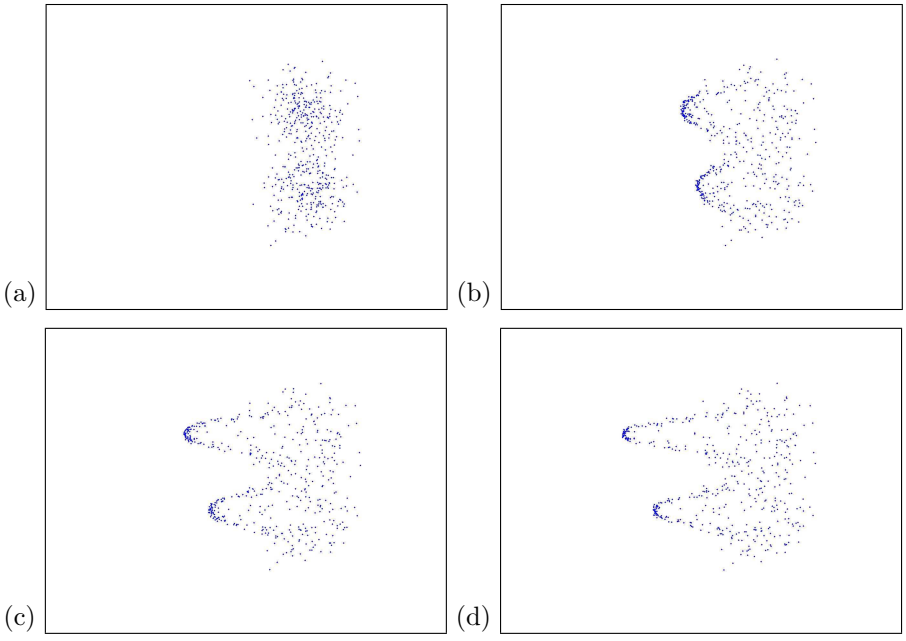

FIGURE 5. A simulation of a bacteria motion towards the light source, on the left. The initial distribution is composed of two Gaussians.

iteration	0	–	100	–	140	–	230	–	280	–	330	–	370	–	400
direction	|	←	|	↓	|	→	|	↑	|	←	|	↓	|	→	|

TABLE 1. Iterations and directions bacteria tend to move to. For example, between iterations 230 and 280 bacteria sense the light from the top of the domain and consequently tend to move upwards.

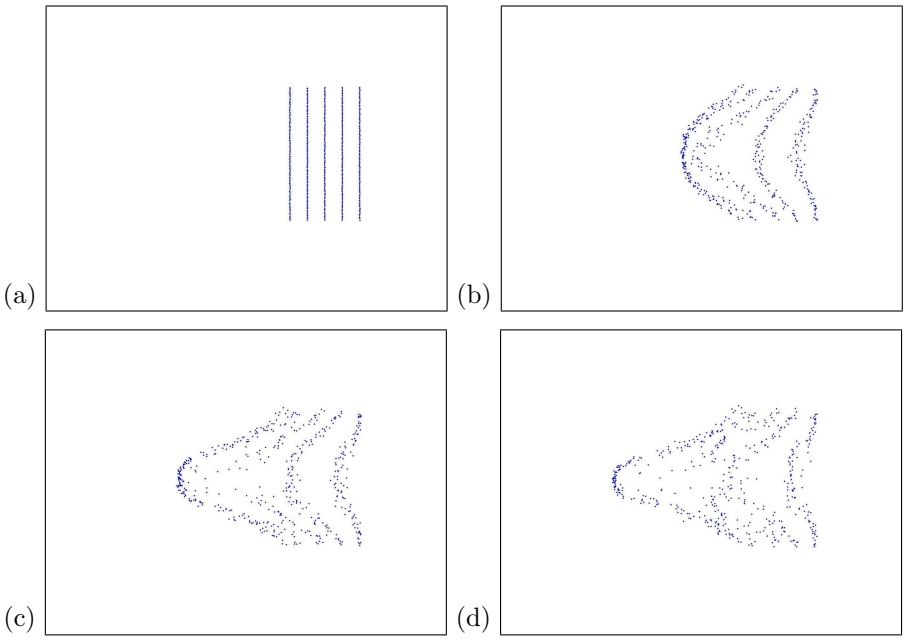

FIGURE 6. A simulation of a bacteria motion towards the light source, on the left. The initial distribution is of particles that are uniformly distributed on lines. The radius of the neighborhood in which the bacteria adjusts its excitation equals to the distance between two vertical lines.

3. **From a Many-Particle System to a System of PDEs.** Our main goal is to derive a continuum model that resembles the stochastic method (1)–(3). The general technique will closely follow the methodology of [18] and [14]. The first step is to create an interacting many-particle system in which all populations are represented by particles. Clearly, the individual bacteria can be easily thought of as particle. To this set we will also add excitation particles and surface particles (that will describe the surface memory effect).

3.1. **A Particle System.** We consider an initial population of approximately N particles that can move in $\mathbb{R}^2$, die, or give birth to new particles. As the initial population size N tends to infinity, we rescale the interaction between individuals in a moderate way. This means that the instantaneous change of a particular particle depends on the configuration of the remaining particles in a neighborhood, which is macroscopically small and microscopically large. That is, the volume of

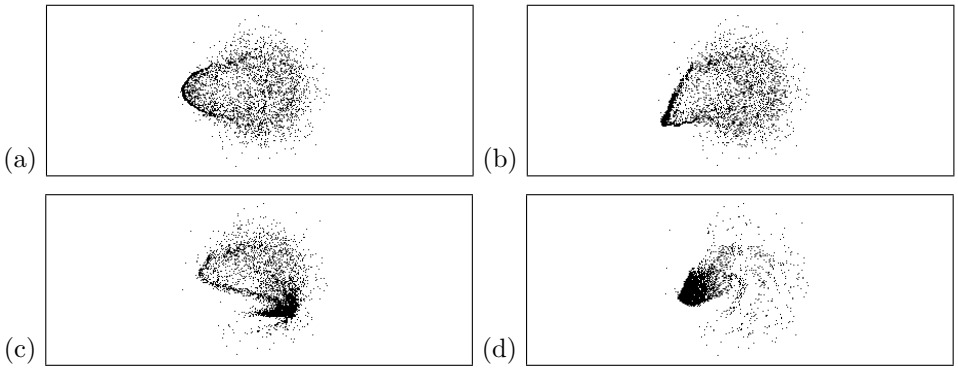

FIGURE 7. Localizing the bacteria by changing the direction of the light source in time. Figures (a)–(d) correspond to iterations 100,140, 230, and 360.

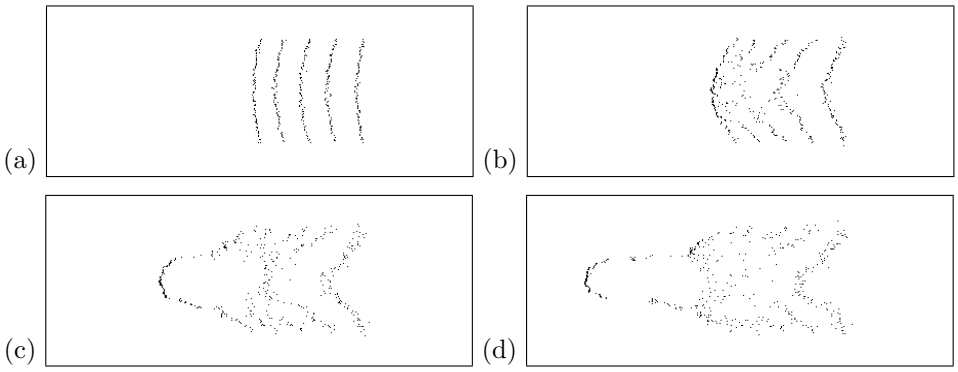

FIGURE 8. A detaching tip shortly after a finger forms.

such neighborhood tends to 0 as $N \to \infty$ and it contains an arbitrarily large number of particles as $N \to \infty$.

Given $N \in \mathbb{N}$, we consider a set of N particles (located in $\mathbb{R}^2$) that are divided into three subpopulations: bacteria, excitation and surface. From now on, these subpopulations will be denoted by the indices u (bacteria), v (excitation), and l (surface). Denote by $M(N, r, t)$, where $r = u, v, l$, the set of all particles belonging to population of type r at time t. We also denote the total number of particles at time t by $M(N, t) = \bigcup_{r=u,v,l} M(N, r, t)$.

For $k \in M(N, t)$, let $P_N^k(t) \in \mathbb{R}^2$ denote the position of particle k at time t. We would like to emphasize that particle k can be either a bacterium particle, and excitation particle, or a surface particle. We then consider the measure valued processes

$$t \to S_{N,r}(t) = \frac{1}{N} \sum_{k \in M(N,r,t)} \delta_{P_N^k}(t), \tag{4}$$

where $r = u, v, l$ and δ_x denotes the Dirac measure at $x \in \mathbb{R}^2$.

Excitation was initially defined as a property of an individual bacteria. Hence, excitation particles should be associated with a particular bacterium. We therefore

have to be particularly careful with the numbering of the excitation particles in the set $M(N,v,t)$. To that end, define $M_w(N,v,t) \subset M(N,v,t)$ as the set of excitation particles that are associated with bacterium $w \in M(N,u,t)$. For any bacterium $w \in M(N,u,t)$ we can then define the measure valued process

$$t \to S_{N,v,w}(t) = \sum_{k \in M_w(N,v,t)} \delta_{P_N^k}(t). \tag{5}$$

Equation (5) is the sum over all the excitation particles that are associated with that bacterium. Note that since $\{M_w(N,v,t)\}_{w \in M(N,u,t)}$ is a partition of $M(N,v,t)$, then $S_{N,v}(t) = \frac{1}{N} \sum_{w \in M(N,u,t)} S_{N,v,w}(t)$.

3.2. **Densities.** We now introduce smoothed versions of the empirical processes above. For a fixed symmetric and sufficiently smooth function W_1 (see [14] for technical conditions on this function), let

$$W_N(x) = \alpha_N^2 W_1(\alpha_N x), \qquad \hat{W}_N(x) = \hat{\alpha}_N^2 W_1(\hat{\alpha}_N x),$$

where $\alpha_N = N^{\alpha/2}$ and $\hat{\alpha}_N = N^{\hat{\alpha}/2}$ for fixed scaling exponents α and $\hat{\alpha}$. We also introduce a sequence $\delta_N = N^{-\delta}$. Given an arbitrarily small $\rho > 0$, we assume α, $\hat{\alpha}$, and δ satisfy

$$\hat{\alpha} \leq \frac{\delta}{3} \quad \text{and} \quad 2\delta(1+2\rho) < \alpha < \frac{2}{5} \tag{6}$$

We are now ready to define for $r = u, v, l$

$$\begin{aligned} s_{N,r}(t,x) &= (S_{N,r}(t) * W_N * W_N)(x), \\ \hat{s}_{N,r}(t,x) &= (S_{N,r}(t) * W_N * \hat{W}_N)(x), \end{aligned} \tag{7}$$

and, for $w \in M(N,v,t)$,

$$\begin{aligned} s_{N,v,w}(t,x) &= (S_{N,v,w}(t) * W_N * W_N)(x), \\ \hat{s}_{N,v,w}(t,x) &= (S_{N,v,w}(t) * W_N * \hat{W}_N)(x). \end{aligned} \tag{8}$$

The functions defined in (7) and (8) formally represent the density or concentration of each subpopulation near x at time t. We introduce two density versions of each type (s and $\hat{s}$) for technical reasons that will be made clear later. A more thorough discussion and technical details can be found in [14]. Finally, we define the following auxiliary functions that will play a major role in the analysis below

$$\begin{aligned} V_N(x) &= (W_N * W_N)(x), \\ h_{N,r}(t,x) &= (S_{N,r}(t) * W_N)(x), \end{aligned} \tag{9}$$

for $r = u, v, l$. Note that the definition (9) implies that $s_{N,r}(t,x) = (h_{N,r}(t) * W_N)(x)$ and $\hat{s}_{N,r}(t,x) = (h_{N,r}(t) * \hat{W}_N)(x)$.

3.3. **Dynamics.** Existing particles can move (in $\mathbb{R}^2$), and they can also cause discontinuous changes to the population, i.e., they can die or give birth to new particles. We start with describing the motion of particles. In what follows, $\{W^k(t)\}_{k \in M(N,t)}$ are independent 2-dimensional Brownian motions. For the bacteria particles we let (for $t \geq 0$)

$$\begin{aligned} dP_N^k(t) =& g\left(\hat{s}_{N,v,k}(t, P_N^k(t)), \hat{s}_{N,l}(t, P_N^k(t)), \nabla s_{N,l}(t, P_N^k(t))\right) dt + \sqrt{2\mu} dW^k(t) \\ :=& g_N^k\left(t, P_N^k(t)\right) dt + \sqrt{2\mu} dW^k(t), \qquad \forall k \in M(N,u,t). \end{aligned} \tag{10}$$

Here, $g_N^k(t,x) = g\left(\hat{s}_{N,v,k}(t,x), \hat{s}_{N,l}(t,x), \nabla s_{N,l}(t,x)\right)$ (compare with (3)). The excitation particles move together with the bacterium they are associated with. Hence, we impose

$$dP_N^k(t) = dP_N^w(t), \qquad \forall k \in M_w(N,v,t). \tag{11}$$

Finally, for the surface memory particles, we have

$$dP_N^k(t) = \sqrt{2\eta} dW^k(t), \qquad \forall k \in M(N,l,t), \tag{12}$$

We assume that η is a small positive constant, so that the surface memory effect diffuses at a slow rate.

We assume that any bacteria particle $k \in M(N,u,t)$ at position $P_N^k(t) = y$ may induce discontinuous changes in the excitation (v) and surface (l) subpopulations; namely they give birth to surface (type l) particles, with intensity $\lambda_N(t,y)$, and they give birth to excitation (type v) particles, with intensity $\beta_{N,k}(t,y)$. We also assume that any excitation particle, $k \in M(N,v,t)$ at position $P_N^k(t) = y$, may cause the death of excitation particles, with intensity $\gamma_{N,k}(t,y)$. (This is equivalent to saying that the death rate of the excitation particles is proportional to the density of these particles). These intensities are assumed to depend on the densities of the N-particle system, i.e.,

$$\begin{aligned} \beta_{N,k}(t,x) &= \beta(\hat{s}_{N,v,k}(t,x), \hat{s}_{N,u}(t,x), \hat{s}_{N,v}(t,x)), \\ \gamma_{N,k}(t,x) &= \gamma(\hat{s}_{N,v,k}(t,x), \hat{s}_{N,u}(t,x), \hat{s}_{N,v}(t,x)), \\ \lambda_N(t,x) &= \lambda(\hat{s}_{N,u}(t,x), \hat{s}_{N,l}(t,x)). \end{aligned} \tag{13}$$

These birth and death processes are given as

$$\begin{aligned} \beta_N^k(t) &= Q_N^{\beta,k}\left(\int_0^t \mathbb{1}_{M(N,u,\tau)}(k)\beta_{N,k}(\tau, P_N^k(\tau))d\tau\right), \\ \gamma_N^k(t) &= Q_N^{\gamma,k}\left(\int_0^t \mathbb{1}_{M(N,v,\tau)}(k)\gamma_{N,k}(\tau, P_N^k(\tau))d\tau\right), \\ \lambda_N^k(t) &= Q_N^{\lambda,k}\left(\int_0^t \mathbb{1}_{M(N,l,\tau)}(k)\lambda_N(\tau, P_N^k(\tau))d\tau\right), \end{aligned} \tag{14}$$

where $Q_N^{\cdot}$ are independent standard Poisson processes. Thus the point processes $\beta_N^k(t)$, $\gamma_N^k(t)$, $\lambda_N^k(t)$ for a jump of size 1 at time t, have intensities $\mathbb{1}_{M(N,u,\tau)}(k)\beta_{N,k}(t, P_N^k(t))$, $\mathbb{1}_{M(N,u,t)}(k)\gamma_{N,k}(t, P_N^k(t))$, and $\mathbb{1}_{M(N,u,t)}(k)\lambda_N(t, P_N^k(t))$.

3.4. **The Limit Dynamics.** In this section we present a heuristic derivation of the limit dynamics of the particle system (10)–(14). The idea is to use Itô's formula on the processes (10), (11) and (12) to obtain integral systems for $S_{N,r}(t)$, $r = u, v, l$. At this point we take the limit when $N \to \infty$ and arrive at an integral system for the densities $r(t,\cdot)$ corresponding to $S_{N,r}(t)$. The *phototaxis system* follows after integrating by parts the limit integral system. At this stage, the transition to the limit densities will be formal. This connection will be rigorously established in the following sections.

Using Itô's formula on (10), we obtain for $f \in C_b^{1,2}(\mathbb{R}^+ \times \mathbb{R}^2)$ and bacterium $k \in M(N,u,t)$,

$$\begin{aligned} f\left(t, P_N^k(t)\right) =& f\left(0, P_N^k(0)\right) + \int_0^t \sqrt{2\mu} \nabla f\left(\tau, P_N^k(\tau)\right) \cdot dW^k(t) \\ &+ \int_0^t \Big[\nabla f\left(\tau, P_N^k(\tau)\right) \cdot g_N^k\left(\tau, P_N^k(\tau)\right) \\ &+ \partial_\tau f\left(\tau, P_N^k(\tau)\right) + \mu \Delta f\left(\tau, P_N^k(\tau)\right) \Big] d\tau. \end{aligned} \tag{15}$$

In order to simplify (15) we define the functional $T_N^k \colon C_b^{1,2}(\mathbb{R}^+ \times \mathbb{R}^2) \to \mathbb{R}$ by

$$T_N^k(\varphi) = \nabla \varphi\left(\tau, P_N^k(\tau)\right) \cdot g_N^k\left(\tau, P_N^k(\tau)\right) + \partial_\tau \varphi\left(\tau, P_N^k(\tau)\right) + \mu \Delta \varphi\left(\tau, P_N^k(\tau)\right). \tag{16}$$

Thus, (15) reads

$$f\left(t, P_N^k(t)\right) = f\left(0, P_N^k(0)\right) + \int_0^t T_N^k(f) d\tau + \int_0^t \sqrt{2\mu} \nabla f\left(\tau, P_N^k(\tau)\right) \cdot dW^k(t). \tag{17}$$

Let $\langle \mu, f \rangle = \int_{\mathbb{R}^2} f(x) \mu(dx)$ for any measure μ and real-valued function f in $\mathbb{R}^2$. In order to study the limit behavior of the bacteria particles, we are interested in computing $\langle S_{N,r}(t), f(t,\cdot) \rangle$. Since there are no births or deaths of type u particles,

$$\begin{aligned} \langle S_{N,u}(t), f(t,\cdot) \rangle =& \langle S_{N,u}(0), f(0,\cdot) \rangle + \frac{1}{N} \int_0^t \sum_{k \in M(N,u,\tau)} T_N^k(f) d\tau \\ &+ \frac{1}{N} \int_0^t \sum_{k \in M(N,u,\tau)} \sqrt{2\mu} \nabla f\left(\tau, P_N^k(\tau)\right) \cdot dW^k(t) \end{aligned} \tag{18}$$

For the excitation particles, i.e., $k \in M(N,v,t)$, we have to take into account birth and decay. The motion of the excitation particles follows the motion of the bacteria particles (see (11)). Thus

$$\begin{aligned} \langle S_{N,v}(t), f(t,\cdot) \rangle =& \frac{1}{N} \sum_{k \in M(N,v,t)} f\left(t, P_N^k(t)\right) + \text{birth/decay terms} \\ =& \frac{1}{N} \sum_{k \in M(N,u,t)} S_{N,v,w}(\tau)\left(P_N^k(\tau)\right) f\left(t, P_N^k(t)\right) + \text{birth/decay terms}. \end{aligned} \tag{19}$$

Hence,

$$\begin{aligned} \langle S_{N,v}(t), f(t,\cdot) \rangle =& \langle S_{N,v}(0), f(0,\cdot) \rangle + \frac{1}{N} \int_0^t \sum_{k \in M(N,u,\tau)} S_{N,v,w}(\tau)\left(P_N^k(\tau)\right) T_N^k(f) d\tau \\ &+ \frac{1}{N} \int_0^t \sum_{k \in M(N,u,\tau)} S_{N,v,w}(\tau)\left(P_N^k(\tau)\right) \sqrt{2\mu} \nabla f\left(\tau, P_N^k(\tau)\right) \cdot dW^k(t) \\ &+ \frac{1}{N} \int_0^t \sum_{k \in M(N,u,\tau)} f\left(\tau, P_N^k(\tau)\right) \beta_N^k(d\tau) - \frac{1}{N} \int_0^t \sum_{k \in M(N,v,\tau)} f\left(\tau, P_N^k(\tau)\right) \gamma_N^k(d\tau). \end{aligned} \tag{20}$$

Finally, for the surface particles we have (see (12)):

$$\begin{aligned}\langle S_{N,l}(t), f(t,\cdot)\rangle = \langle S_{N,l}(0), f(0,\cdot)\rangle &+ \frac{1}{N}\int_0^t \sum_{k\in M(N,l,\tau)} T_N^k(f)d\tau \\ &+ \frac{1}{N}\int_0^t \sum_{k\in M(N,l,\tau)} \sqrt{2\eta}\nabla f\left(\tau, P_N^k(\tau)\right)\cdot dW^k(t) \\ &+ \frac{1}{N}\int_0^t \sum_{k\in M(N,u,\tau)} f\left(\tau, P_N^k(\tau)\right)\lambda_N^k(d\tau).\end{aligned} \tag{21}$$

To deal with the random components of the dynamics, we introduce the processes

$$\begin{aligned}M_r^N(t,f) &= \frac{1}{N}\int_0^t \sum_{k\in M(N,r,t)} \sqrt{2\mu}\nabla f\left(\tau, P_N^k(\tau)\right)\cdot dW^k(t), \qquad r=u,v,l, \\ M_{v,\gamma}^N(t,f) &= \frac{1}{N}\int_0^t \sum_{k\in M(N,u,\tau)} f\left(\tau, P_N^k(\tau)\right)\left(\gamma_N^k(d\tau) - \gamma_{N,k}\left(\tau, P_N^k(\tau)\right)d\tau\right), \\ M_{v,\beta}^N(t,f) &= \frac{1}{N}\int_0^t \sum_{k\in M(N,v,\tau)} f\left(\tau, P_N^k(\tau)\right)\left(\beta_N^k(d\tau) - \beta_{N,k}\left(\tau, P_N^k(\tau)\right)d\tau\right), \\ M_{l,\lambda}^N(t,f) &= \frac{1}{N}\int_0^t \sum_{k\in M(N,u,\tau)} f\left(\tau, P_N^k(\tau)\right)\left(\lambda_N^k(d\tau) - \lambda_N\left(\tau, P_N^k(\tau)\right)d\tau\right).\end{aligned} \tag{22}$$

The processes defined in (22) are martingales with respect to the natural filtration generated by the processes $t \to \left(P_N^k(t), \mathbb{1}_{M(N,r,t)}(k)\right)\mathbb{1}_N^k(t)$ where $\mathbb{1}_N^k(t)$ is the indicator function of the lifetime of individual k. If we assume that the quadratic variation of these martingales tends to 0 as $N\to\infty$, they can be neglected when passing to the limit dynamics.

From Section 3.2, we see that in the sense of distributions,

$$\lim_{N\to\infty} W_N = \lim_{N\to\infty} \hat{W}_N = \delta_0.$$

For $r=u,v,l$ and $t\geq 0$ we assume that in some sense (similarly to [18] and [14]),

$$\lim_{N\to\infty} S_{N,r}(t) = S_r(t),$$

where the measures $S_r(t)$ have a smooth density $r(t,\cdot)$. It follows that

$$\lim_{N\to\infty} s_{N,r}(t,\cdot) = \lim_{N\to\infty} \hat{s}_{N,r}(t,\cdot) = r(t,\cdot),$$

and

$$\lim_{N\to\infty} \nabla s_{N,r}(t,\cdot) = \lim_{N\to\infty} \nabla \hat{s}_{N,r}(t,\cdot) = \nabla r(t,\cdot).$$

Let $u_0(\cdot)$, $v_0(\cdot)$ and $l_0(\cdot)$ be the densities of $S_u(0)$, $S_v(0)$ and $S_l(0)$. Define $\lambda_\infty(\tau,x) = \lambda(u(\tau,x), l(\tau,x))$ as the growth rate of surface memory at $x\in\mathbb{R}^2$ at time τ. In order to define g_∞, β_∞ and γ_∞, we assume that as $N\to\infty$, the total excitations of bacteria (w and $\tilde{w}$) that are close with respect to the size of the interaction domain should be close to each other. That is, if $|P_N^w(t) - P_N^{\tilde{w}}(t)|$ is small compared to the domain of interaction then

$$|M_w(N,v,t)| \simeq |M_{\tilde{w}}(N,v,t)|.$$

Thus, in the limit as $N \to \infty$, $S_{N,v,w}(t)$ should be approximated by the number of excitation particles at $P_N^w(t)$ divided by the number of bacteria particles at $P_N^w(t)$, i.e.

$$S_{N,v,w}(t)(P_N^w) \simeq \frac{\sum_{k\in S_v(N,t)} \delta_{P_N^k}(P_N^w)}{\sum_{k\in S_u(N,t)} \delta_{P_N^k}(P_N^w)} = \frac{S_{N,v}(t)(P_N^w)}{S_{N,u}(t)(P_N^w)},$$

which, in turn, implies that

$$\lim_{N\to\infty} \hat{s}_{N,v,x}(t) = \frac{v(t,x)}{u(t,x)}.$$

Hence, we get $g_\infty(\tau,\cdot) = g\left(\frac{v(\tau,\cdot)}{u(\tau,\cdot)}, \nabla l(\tau,\cdot), \nabla u(\tau,\cdot)\right)$, $\gamma_\infty(\tau,\cdot) = \gamma\left(\frac{v(\tau,\cdot)}{u(\tau,\cdot)}, u(\tau,\cdot), v(\tau,\cdot)\right)$, and $\beta_\infty(\tau,\cdot) = \beta\left(\frac{v(\tau,\cdot)}{u(\tau,\cdot)}, u(\tau,\cdot), v(\tau,\cdot)\right)$. We can now formally take the limit and obtain

$$\begin{aligned}
\langle u(t,\cdot), f(t,\cdot)\rangle =& \langle u_0(\cdot), f(0,\cdot)\rangle \\
&+ \int_0^t \big\langle u(t,\cdot), \nabla f(\tau,\cdot)\cdot g_\infty(\tau,\cdot) + \partial_\tau f(\tau,\cdot) + \mu\Delta f(\tau,\cdot)\big\rangle d\tau \\
\langle v(t,\cdot), f(t,\cdot)\rangle =& \langle v_0(\cdot), f(0,\cdot)\rangle \\
&+ \int_0^t \big\langle v(t,\cdot), \nabla f(\tau,\cdot)\cdot g_\infty(\tau,\cdot) + \partial_\tau f(\tau,\cdot) + \mu\Delta f(\tau,\cdot)\big\rangle d\tau \\
&+ \int_0^t \langle u(t,\cdot), \beta_\infty(\tau,\cdot) f(\tau,\cdot)\rangle\, d\tau - \int_0^t \langle v(t,\cdot), \gamma_\infty(\tau,\cdot) f(\tau,\cdot)\rangle d\tau \\
\langle l(t,\cdot), f(t,\cdot)\rangle =& \langle l_0(\cdot), f(0,\cdot)\rangle \\
&+ \int_0^t \big\langle l(t,\cdot), \partial_\tau f(\tau,\cdot) + \eta\Delta f(\tau,\cdot)\big\rangle d\tau \\
&+ \int_0^t \langle u(t,\cdot), \lambda_\infty(\tau,\cdot) f(\tau,\cdot)\rangle\, d\tau.
\end{aligned} \tag{23}$$

Integrating (23) by parts we obtain the system

$$\begin{cases}
\partial_t u =& \mu\Delta u - \nabla\cdot\big(g(v/u, l, \nabla l)u\big), \\
\partial_t v =& \mu\Delta v - \nabla\cdot\big(g(v/u, l, \nabla l)v\big) + \beta(v/u, u, v)u - \gamma(v/u, u, v)v, \\
\partial_t l =& \eta\Delta l + \lambda(u, l)u,
\end{cases} \tag{24}$$

which we rewrite as

$$\begin{cases}
\partial_t u =& \mu\Delta u - \nabla\cdot\big(g(u, v, l, \nabla l)u\big), \\
\partial_t v =& \mu\Delta v - \nabla\cdot\big(g(u, v, l, \nabla l)v\big) + \beta(u, v)u - \gamma(u, v)v, \\
\partial_t l =& \eta\Delta l + \lambda(u, l)u.
\end{cases} \tag{25}$$

with a new function g that replaces the function g in (24). From now on, we will refer to the system (25) as the *phototaxis system*.

Remark 5. The structure of the system (25) is not surprising, We expect the rate of change on bacteria density u to be given by a diffusion part (originating from the Brownian motion) plus an advection term that captures the sensitivity to light and the external substance. Similarly, the *excitation* density v, can be expected to follow the same motion pattern as u and hence an identical velocity, with the

addition of birth and decay terms. The surface is marked proportionally to the motion of the bacteria, with a weak diffusion term.

Remark 6. The phototaxis system (25) is similar to the classical chemotaxis system

$$\begin{cases} \partial_t u = \mu\Delta u - \nabla\cdot\big(\chi(u,v)u\nabla v\big) \\ \partial_t l = \eta\Delta l + \lambda(u,l)u - \kappa(u,l)l \end{cases} \tag{26}$$

where u is the bacteria density and v is the density of chemo-attractant. The main difference in our case is the existence of an internal property, which shows up in the system (25) as a quantity that closely follows the dynamics of the bacteria u (plus the additional birth and decay terms).

Remark 7. Our derivation is based on the assumption that, as $N\to\infty$, $|M_w(N,v,t)| \simeq |M_{\tilde{w}}(N,v,t)|$ if $P_N^w(t) = P_N^{\tilde{w}}(t)$. That is, as $N\to\infty$, our model looks like a reaction-diffusion system, which allows us to use the methods discussed in [18] and [14]. As mentioned above, when rescaling the interaction in a moderate way, we are looking at neighborhoods that are microscopically large. Hence, as $N\to\infty$, we expect to have an arbitrarily large number of individuals in such neighborhoods.

Remark 8. Comparing with the model introduced in Section 2.2, arriving at possible functions for g and λ is fairly easy. In fact one can use function q with minor modifications in place of g. For β and γ one needs to be somewhat careful as these functions regulate the dynamics of v. In particular β and γ must lead to $\frac{v}{u}$ bounded, and well defined as u approaches 0. A possible choice is $\beta(u,v) = 0$ whenever $v > Cu$ for some fixed constant C, and $\gamma(u,v)$ large enough when u approaches zero in order to guarantee smoothness of $\frac{v}{u}$. This choice for β guarantees boundedness of $\frac{v}{u}$, while the choice for γ ensures v approaches zero sufficiently fast when u approaches zero.

3.5. **Limit Theorems.** In this section we proceed with the formal approach corresponding to the description given in Sec. 3.4. This approach follows closely the work of Stevens [18], and Oelschläger [14]. The idea is to consider an intermediate system (see (27) below), and show the solution for this system is in some sense close to both the solution for the phototaxis system and the limit of $S_{N,r}$ as $N\to\infty$. The precise statements are given in Theorems 3.1, 3.2, and 3.3. Theorem 3.1 asserts that the solution for (27) converges to the solution of the phototaxis system in the $|\cdot|_{[0,T]}$ introduced below. Theorem 3.2 shows that the difference between the solution for (27) and a smoothed version of the processes $S_{N,r}$ is approaching zero as $N\to\infty$. Finally, Theorem 3.3 combines the results from the previous theorems to conclude the desired result.

Before stating the main results, we will outline some technical assumptions. We assume that W_1 is a symmetric probability density (as in [18]). These are reasonable assumptions as a Gaussian probability density satisfies them. Since $s_{N,r}$ and $\hat{s}_{N,r}$ are given by a convolution with W_N and $\hat{W}_N$, we have the estimate

$$\left|\left|\frac{\partial^{k_1+k_2}}{(\partial x_1)^{k_1}(\partial x_1)^{k_2}}\hat{s}_{N,r}\right|\right|_{C^0} \le C(k_1,k_2)\langle S_N(t),1\rangle\hat{\alpha}_N^{2+k_1+k_2},$$

where $k_1,k_2\in\mathbb{N}$, $t\ge 0$.

We also assume that the following quantities are positive, $\mu,\eta,\sigma>0$; that the function g is continuously differentiable and bounded together with its derivatives; that β,γ,λ are continuously differentiable and bounded together with its derivatives;

and that $u_0, v_0, l_0 \in C_b^\infty(\mathbb{R}^2)$ with $\langle u_0, \psi\rangle, \langle v_0, \psi\rangle, \langle l_0, \psi\rangle \leq C$ for $\psi(x) = \log(2 + x^2), x \in \mathbb{R}^2$. The form of this function as identical to the one in [18]. Finally, we assume that for some $T > 0$, the phototaxis system (24) has a unique positive solution $u, v, l \in C_b^\infty([0,T] \times \mathbb{R}^2, \mathbb{R}) \cap C^0([0,T], L_2(\mathbb{R}^2))$ such that v/u is also in $C_b^\infty([0,T] \times \mathbb{R}^2, \mathbb{R}) \cap C^0([0,T], L_2(\mathbb{R}^2))$.

Denote by $||\cdot||_2$ the L^2-norm in $\mathbb{R}^2$ and define

$$|f|_{[0,T]} = \sup_{t \leq T} ||f||_2^2 + \int_0^T ||\nabla f||_2^2 \, dt,$$

for any function $f \in C^0([0,T], L^2(\mathbb{R}^2)) \cap L^2([0,T], L^2(\mathbb{R}^2))$. We also define for all positive measures ν_1, ν_2 on $\mathbb{R}^2$,

$$d(\nu_1, \nu_2) = \sup\{\langle \nu_1 - \nu_2, f\rangle \colon f \in C_b^1(\mathbb{R}^2), ||f||_{C^0} + ||\nabla f||_{C^0} \leq 1\}.$$

We are now ready to consider the system

$$\begin{cases} \partial_t \hat{u}_N = \nabla \cdot \big(\mu \nabla \hat{u}_N - \hat{g}_N \hat{u}_N\big), \\ \partial_t \hat{v}_N = \nabla \cdot \big(\mu \nabla \hat{v}_N - \hat{g}_N \hat{v}_N\big) + \hat{\beta}_N \hat{u}_N - \hat{\gamma}_N \hat{v}_N, \\ \partial_t \hat{l}_N = \eta \Delta \hat{l}_N + \hat{\lambda}_N \hat{u}_N, \end{cases} \tag{27}$$

subject to the initial data $\hat{u}_N(0,x) = \hat{u}_{N0}(x)$, $\hat{v}_N(0,x) = \hat{v}_{N0}(x)$, and $\hat{l}_N(0,x) = \hat{l}_{N0}(x)$. Here, $\hat{g}_N(t,x) = g\big((\hat{u}_N(t,\cdot) * \hat{W}_N)(x), (\hat{v}_N(t,\cdot) * \hat{W}_N)(x), (\hat{l}_N(t,\cdot) * \hat{W}_N)(x), \nabla(\hat{u}_N(t,\cdot) * \hat{W}_N)(x)\big)$, $\beta_N(t,x) = \beta\big((\hat{u}_N(t,\cdot) * \hat{W}_N)(x), (\hat{v}_N(t,\cdot) * \hat{W}_N)(x)\big)$, and $\gamma_N(t,x)$, $\lambda_N(t,x)$ are defined in a similar way. We assume that the system (27) has a unique positive solution $\hat{u}_N, \hat{v}_N, \hat{l}_N \in C_b^{1,\infty}([0,T] \times \mathbb{R}^2, \mathbb{R}) \cap C^0([0,T], L_2(\mathbb{R}^2))$ such that $\hat{v}_N/\hat{u}_N$ also belongs to $C_b^{1,\infty}([0,T] \times \mathbb{R}^2, \mathbb{R}) \cap C^0([0,T], L_2(\mathbb{R}^2))$. Under these conditions, the theorems from [18] that were formulated for the chemotaxis system hold also for the phototaxis system:

Theorem 3.1. *If $\hat{u}_{N0}, \hat{v}_{N0}, \hat{l}_{N0} \in C_b^\infty(\mathbb{R}^2)$ and*

$$\lim_{N \to \infty} ||\hat{u}_{N0} - u_0||_2^2 + ||\hat{v}_{N0} - v_0||_2^2 + ||\hat{l}_{N0} - l_0||_2^2 = 0, \tag{28}$$

then the solutions for (27) are uniformly bounded with respect to N in the associated norm and

$$\lim_{N \to \infty} |\hat{u}_N - u|_{[0,T]} + |\hat{v}_N - v|_{[0,T]} + |\hat{l}_N - l|_{[0,T]} = 0. \tag{29}$$

Theorem 3.2. *Assume that the initial distributions of particles are converging*

$$\lim_{N \to \infty} P\Big[||h_{N,u}(0,\cdot) - \hat{u}_{N0}||_2^2 + ||h_{N,v}(0,\cdot) - \hat{v}_{N0}||_2^2 + ||h_{N,l}(0,\cdot) - \hat{l}_{N0}||_2^2 \geq \delta_N^{1+2\rho}\Big] = 0, \tag{30}$$

and that the number of particles grows in a controlled way, i.e.,

$$\lim_{n \to \infty} \sup_{N \in \mathbb{N}} P[\langle S_N(0), 1\rangle \geq n] = 0. \tag{31}$$

Then

$$\lim_{N \to \infty} P\Big[|h_{N,u} - \hat{u}_N|_{[0,T]} + |h_{N,v} - \hat{v}_N|_{[0,T]} + |h_{N,l} - \hat{l}_N|_{[0,T]} \geq \delta_N\Big] = 0, \tag{32}$$

where $\hat{u}_N$, $\hat{v}_N$, $\hat{l}_N$ is the unique solution for (27).

Theorem 3.3. *Assume that the initial distribution of particles is controlled in the limit*

$$\lim_{n\to\infty}\sup_{N\in\mathbb{N}} P[\langle S_{N,u}(0),\psi^2\rangle + \langle S_{N,v}(0),\psi^2\rangle + \langle S_{N,l}(0),\psi^2\rangle \geq n] = 0, \tag{33}$$

where $\psi(x) = \log(2+x^2)$. *Then* $S_{N,r}$ *converge in probability to the corresponding densities, i.e., for* $\delta > 0$,

$$\lim_{N\to\infty} P\left[\sup_{t\leq T} d(S_{N,u}(t),u(t,\cdot)) + \sup_{t\leq T} d(S_{N,v}(t),v(t,\cdot)) + \sup_{t\leq T} d(S_{N,l}(t),l(t,\cdot)) \geq \delta\right] = 0. \tag{34}$$

Theorem 3.3 gives us the desired result, i.e., the phototaxis system (24) is the limit as $N\to\infty$ for the particle systems whose dynamics is defined by (10), (11), and (12).

The proofs of these theorems follow the arguments in [18]. The main difference is in the proof of Theorem 3.2. This proof requires adjustments to some of the estimates in [18]. In Section 4 we sketch the proof of Theorem 3.2. We do not provide the proofs for Theorems 3.1 and 3.3 . The proof of Theorem 3.1 is similar to the one for Theorem 3.2, where estimates to $|\hat{r}_N - r|_{[0,T]}$ are obtained in the same way as in Sec. 4.2. Theorem 3.3 is a consequence of the first two theorems, and its proof can be repeated by following the arguments in [18] with minor modifications.

4. **A Sketch of the Proof of Theorem 3.2.** Generally, the proof follows the arguments of [18] with some necessary adjustments that are outlined below. For technical reasons, we will need to consider the following system

$$\begin{cases} \partial_t u_N = \nabla\cdot\big(\mu\nabla u_N - g_N u_N\big), \\ \partial_t v_N = \nabla\cdot\big(\mu\nabla v_N - g_N v_N\big) + \beta_N u_N - \gamma_N v_N, \\ \partial_t l_N = \eta\Delta l_N + \lambda_N u_N, \end{cases} \tag{35}$$

subject to the initial data $u_N(0,x) = u_{N0}(x)$, $v_N(0,x) = v_{N0}(x)$, and $l_N(0,x) = l_{N0}(x)$. Here, $g_N(t,x) = g\left(\hat{s}_{N,v}(t,x)/\hat{s}_{N,u}(t,x), \nabla s_{N,l}(t,x), \nabla s_{N,u}(t,x)\right)$ and $\beta_N(t,x)$, $\gamma_N(t,x)$, and $\lambda_N(t,x)$ are defined analogously. Note that g_N, β_N, γ_N, and λ_N don't depend directly on u_N, v_N, or l_N. This is the phototaxis system with frozen nonlinearities. We assume that this system has a unique regular solution u_N, v_N, l_N.

The system (35) will be used to show that for a suitable stopping time T_N,

$$\lim_{N\to\infty} P\left[|h_{N,u} - u_N|_{[0,T_N]} + |h_{N,v} - v_N|_{[0,T_N]} + |h_{N,l} - l_N|_{[0,T_N]} \geq \delta_N^{1+\rho}\right] = 0.$$

We will also determine that

$$\lim_{N\to\infty} P\left[|u_N - \hat{u}_N|_{[0,T_N]} + |v_N - \hat{v}_N|_{[0,T_N]} + |l_N - \hat{l}_N|_{[0,T_N]} \geq \frac{\delta_N}{2}\right] = 0,$$

and using a triangle inequality, conclude with the desired result of Theorem 3.2.

Following our previous assumptions, we assume that the difference between $\hat{s}_{N,v,u}(t,x)$, $\hat{s}_{N,v}(t,x)/\hat{s}_{N,u}(t,x)$, and $v(t,x)/u(t,x)$ converge to zero sufficiently fast when $N\to\infty$. A consequence of this assumption is that

$$|(g_N^k - g_N)(t,x)| \leq A_N(t,x)\,||\nabla g||_{C^0} \tag{36}$$

where $||A_N||_2 \to 0$ sufficiently fast as $N\to\infty$. The same estimate holds when g is substituted for β or γ. Another consequence of such assumption is that the quantity

$v(t,x)/u(t,x)$ is bounded and goes to zero as $u(t,x)$ goes to zero. In particular, we must have

$$\left|\left|\frac{v(t,x)}{u(t,x)}-\frac{v(t,y)}{u(t,y)}\right|\right|_2^2 \leq C\,||u(t,x)-u(t,y)||_2^2\,. \tag{37}$$

We assume this behavior is valid for both systems (27) and (35). Essentially, such an assumption is reasonable as one expects the excitation to tend to zero (at a certain rate) in location where the density of bacteria also tends to zero.

Due to the hypothesis (31) and the fact that β is a bounded function, we have

$$\lim_{n\to\infty}\sup_{N\in\mathbb{N}} P[\sup_{\tau\leq T}\langle S_N(\tau),1\rangle \geq n] = 0. \tag{38}$$

This means the number of particles is in some sense *controlled* up to time T. Note that the quantity $\langle S_N(\tau),1\rangle$ is the total number of particles at time τ divided by N, so (38) really means that the ratio between the number of particles for the N-system and N is bounded almost surely.

Based on (38), it is natural to consider the following stopping times

$$\tilde{T}_N^n(\omega) = \inf\left\{\tau>0\Big|\sup_{\sigma\leq\tau}\langle S_N(\sigma),1\rangle(\omega) > n\right\}.$$

Note that (38) is valid if one substitutes T with any $\bar{T}<\infty$. In particular, defining[1] $T_N^n := T\wedge\tilde{T}_N^n$, one has $\lim_{n\to\infty}P[T_N^n>T]=1$, so we just need to show that

$$\lim_{N\to\infty} P\left[|h_{N,u}-\hat{u}_N|_{[0,T_N^n]}+|h_{N,v}-\hat{v}_N|_{[0,T_N^n]}+|h_{N,l}-\hat{l}_N|_{[0,T_N^n]}\geq\delta_N\right]=0 \tag{39}$$

in order to conclude with (32). To that end consider the hitting time

$$t_N(\omega)=\left\{\tau>0\;\Big|\;\left(|h_{N,u}-\hat{u}_N|_{[0,\tau]}+|h_{N,v}-\hat{v}_N|_{[0,\tau]}+|h_{N,l}-\hat{l}_N|_{[0,\tau]}\right)(\omega)\geq\delta_N\right\}.$$

For any stopping time $T_0=T_0(\omega)$, denote $[0,T_0]=\{\tau\wedge T_0\colon \tau\geq 0\}$. With this notation and from the definition of t_N we have

$$\begin{aligned}
&P\left[|h_{N,u}-\hat{u}_N|_{[0,T_N^n]}+|h_{N,v}-\hat{v}_N|_{[0,T_N^n]}+|h_{N,l}-\hat{l}_N|_{[0,T_N^n]}\geq\delta_N\right]\\
&=P\left[|h_{N,u}-\hat{u}_N|_{[0,T_N^n\wedge t_N]}+|h_{N,v}-\hat{v}_N|_{[0,T_N^n\wedge t_N]}+|h_{N,l}-\hat{l}_N|_{[0,T_N^n\wedge t_N]}\geq\delta_N\right]\\
&\leq P\left[|h_{N,u}-u_N|_{[0,T_N^n\wedge t_N]}+|h_{N,v}-v_N|_{[0,T_N^n\wedge t_N]}+|h_{N,l}-l_N|_{[0,T_N^n\wedge t_N]}\geq\delta_N^{1+\rho}\right]\\
&+P\left[|u_N-\hat{u}_N|_{[0,T_N^n\wedge t_N]}+|v_N-\hat{v}_N|_{[0,T_N^n\wedge t_N]}+|l_N-\hat{l}_N|_{[0,T_N^n\wedge t_N]}\geq\frac{\delta_N}{2}\right].
\end{aligned}\tag{40}$$

The inequality above comes from using triangle inequality and from noting that for N large, $\delta_N^{1+\rho}=N^{-\delta(1+\rho)}<\frac{N^{-\delta}}{2}=\frac{\delta_N}{2}$. We need to estimate the right side of (40) in order to achieve (39). Those estimates rely on uniform boundedness with respect to N of $\sup_{t\leq T_N^n\wedge t_N}||\hat{s}_{N,r}(t,\cdot)||_{C^2}$. This is a consequence of Theorem 3.1 and was done in [18].

We note that (40) brings the system (35) into play. As mentioned above, the idea for the proof is to show the solution of (35) is close to $h_{N,r}$ and also to the solution to (27). We first look at the first term on the right-hand side of (40). In what follows, $t\leq T_N^n\wedge t_N$.

[1] the notation $\wedge$ means $a\wedge b=\min\{a,b\}$

4.1. **Estimates for $|\mathbf{h_{N,r}} - \mathbf{r_N}|_{[\mathbf{0},\mathbf{T_N^n}\wedge\mathbf{t_N}]}$.** In order to obtain an estimate for the first term on the right-hand side of (40), we will first look at $||h_{N,r}(t,\cdot) - r_N(t,\cdot)||_2^2$, for $r = u, v, l$. We have

$$\begin{aligned} ||h_{N,r}(t,\cdot) - r_N(t,\cdot)||_2^2 = &\langle h_{N,r}(t,\cdot), h_{N,r}(t,\cdot)\rangle - 2\langle h_{N,r}(t,\cdot), r_N(t,\cdot)\rangle \\ &+ \langle r_N(t,\cdot), r_N(t,\cdot)\rangle . \end{aligned} \tag{41}$$

We first note that

$$\begin{aligned} \langle h_{N,r}(t,\cdot), h_{N,r}(t,\cdot)\rangle = &\frac{1}{N^2}\sum_{k,l\in M(N,r,t)} V_N(P_N^k(t) - P_N^l(t)) \\ &+ \begin{array}{l}\text{terms resulting from discontinuities} \\ \text{in the size of population } r.\end{array} \end{aligned} \tag{42}$$

and look at each of the populations u, v, and l. Following the arguments of [18] with the necessary adjustments due to the new terms of the form $g_N^k - g_N$, for the bacteria particles (type-u) one can obtain the upper bound

$$\begin{aligned} &\sup_{t\le\tilde{T}\wedge T_N^n\wedge t_N} ||h_{N,u}(t,\cdot) - u_N(t,\cdot)||_2^2 \le ||h_{N,u}(0,\cdot) - u_N(0,\cdot)||_2^2 \\ &- 2\int_0^{\tilde{T}\wedge T_N^n\wedge t_N} \mu \left|\left|\nabla\Big(h_{N,u}(\tau,\cdot) - u_N(\tau,\cdot)\Big)\right|\right|_2^2 d\tau \\ &+ C\tilde{C}\int_0^{\tilde{T}\wedge T_N^n\wedge t_N} \sup_{\sigma\le\tau} ||h_{N,u}(\sigma,\cdot)A_N(\sigma,\cdot)||_2^2\, d\tau \\ &+ C\tilde{C}\int_0^{\tilde{T}\wedge T_N^n\wedge t_N} \sup_{\sigma\le\tau} ||h_{N,u}(\sigma,\cdot) - u_N(\sigma,\cdot)||_2^2\, d\tau \\ &+ \frac{C}{\tilde{C}}\int_0^{\tilde{T}\wedge T_N^n\wedge t_N} ||\nabla\left(h_{N,u}(\tau,\cdot) - u_N(\tau,\cdot)\right)||_2^2\, d\tau \\ &+ C\tilde{C}\tilde{T}\langle S_{N,u}(0),1\rangle^2 \exp(-C'\alpha_N^\varepsilon) + C\tilde{C}\alpha_N^{2\varepsilon-2}\int_0^{\tilde{T}\wedge T_N^n\wedge t_N} ||u_N(\tau,\cdot)||_2^2\, d\tau \\ &+ \frac{C}{N}\alpha_N^4\tilde{T}\langle S_{N,u}(0),1\rangle + \sup_{t\le\tilde{T}\wedge T_N^n\wedge t_N} |M_{N,u}(t)| . \end{aligned} \tag{43}$$

Here,

$$M_{N,u}(t) = \frac{2}{N}\int_0^t \sum_{k\in M(N,u,\tau)} \sqrt{2\mu}\nabla\Big(s_{N,u} - u_N(\tau,\cdot) * W_N\Big)\left(\tau, P_N^k(\tau)\right)\cdot dW^k(\tau)$$

is a martingale with respect to $\{\mathcal{F}_{\tau\wedge T_N^n\wedge t_N}\}_{\tau\in[0,T]}$.

Note that on the RHS of (43), besides the terms in $||h_{N,r}(t,\cdot) - r_N(t,\cdot)||_2^2$ and $||\nabla\left(h_{N,u}(t,\cdot) - u_N(t,\cdot)\right)||_2^2$, all the other terms tend to zero as $N\to\infty$. This happens due to (36), the initial choice for the coefficients α_N, and the martingale inequality above.

For the excitation particles (type-v), the following estimate holds:

$$
\begin{aligned}
&\sup_{t\leq\tilde{T}\wedge T_N^n\wedge t_N}||h_{N,v}(t,\cdot)-v_N(t,\cdot)||_2^2\leq||h_{N,v}(0,\cdot)-v_N(0,\cdot)||_2^2\\
&-2\int_0^{\tilde{T}\wedge T_N^n\wedge t_N}\mu\left|\left|\nabla\Big(h_{N,v}(\tau,\cdot)-v_N(\tau,\cdot)\Big)\right|\right|_2^2d\tau\\
&+C\int_0^{\tilde{T}\wedge T_N^n\wedge t_N}\tilde{C}\sup_{\sigma\leq\tau}||h_{N,u}(\sigma,\cdot)A_N(\sigma,\cdot)||_2^2+\sup_{\sigma\leq\tau}||A_N(\sigma,\cdot)*W_N||_2^2\,d\tau\\
&+C\tilde{C}\int_0^{\tilde{T}\wedge T_N^n\wedge t_N}\sup_{\sigma\leq\tau}||h_{N,u}(\sigma,\cdot)-u_N(\sigma,\cdot)||_2^2\,d\tau+C\int_0^{\tilde{T}\wedge T_N^n\wedge t_N}\sup_{\sigma\leq\tau}||h_{N,v}(\sigma,\cdot)-v_N(\sigma,\cdot)||_2^2\,d\tau\\
&+\frac{C}{\tilde{C}}\int_0^{\tilde{T}\wedge T_N^n\wedge t_N}||\nabla\left(h_{N,u}(\tau,\cdot)-u_N(\tau,\cdot)\right)||_2^2\,d\tau\\
&+C\tilde{C}\tilde{T}\sup_{\tau\leq\tilde{T}}\langle S_N(\tau\wedge T_N^n),1\rangle^2\exp(-C'\alpha_N^{\varepsilon})+C\tilde{C}\alpha_N^{2\varepsilon-2}\int_0^{\tilde{T}\wedge T_N^n\wedge t_N}||v_N(\tau,\cdot)||_2^2\,d\tau\\
&+\frac{C}{N}\alpha_N^4\tilde{T}\sup_{\tau\leq\tilde{T}}\langle S_N(\tau\wedge T_N^n),1\rangle+C\frac{\alpha_N^2}{N}\tilde{T}\sup_{\tau\leq\tilde{T}}\langle S_{N,v}(\tau\wedge T_N^n),1\rangle\\
&+\sup_{t\leq\tilde{T}\wedge T_N^n\wedge t_N}|M_{N,v}(t)|+\sup_{t\leq\tilde{T}\wedge T_N^n\wedge t_N}\left|M_{N,v}^{\beta,0}(t)\right|+\sup_{t\leq\tilde{T}\wedge T_N^n\wedge t_N}\left|M_{N,v}^{\beta,1}(t)\right|\\
&+\sup_{t\leq\tilde{T}\wedge T_N^n\wedge t_N}\left|M_{N,v}^{\gamma,0}(t)\right|+\sup_{t\leq\tilde{T}\wedge T_N^n\wedge t_N}\left|M_{N,v}^{\gamma,1}(t)\right|.
\end{aligned}
\tag{44}
$$

Here, $M_{N,v}^{\beta,0}(t)$ is a martingale with respect to the filtration $\{\mathcal{F}_{\tau\wedge T_N^n\wedge t_N}\}_{\tau\in[0,T]}$. defined as

$$
M_{N,v}^{\beta,0}(t)=\frac{1}{N^2}\int_0^t\sum_{k\in M(N,u,\tau)}V_N(0)\left(\beta_N^k(d\tau)-\beta_{N,k}\left(\tau,P_N^k(\tau)\right)d\tau\right).
$$

Finally, for the type-l particles, from the dynamics defined in Sec. 3.3, after given birth type-l particles behave in a similar way to type-v particles except for the terms involving g. This means the estimates for population l are exactly the same estimates as the ones obtained for type-v particles without the terms in g and without the death terms.

Combining the estimates for all three types of particles (u, v, and l), for $\varepsilon<\frac{1}{2}$, $\tilde{C}$ large enough, and N large we conclude

$$
\sum_{r=u,v,l}\left[\sup_{t\leq\tilde{T}\wedge T_N^n\wedge t_N}||h_{N,r}(t,\cdot)-r_N(t,\cdot)||_2^2+\int_0^{\tilde{T}\wedge T_N^n\wedge t_N}\left|\left|\nabla\Big(h_{N,r}(\tau,\cdot)-r_N(\tau,\cdot)\Big)\right|\right|_2^2\right]
$$

is less or equal than the sum of the right hand sides of (43), (44), and the expression that is the analog of (44) for type-l particles. Using Gronwall's inequality on this expression one gets, for some new $\bar{C}$ depending on n, T, and all the previous

constants,

$$\begin{aligned}
&P\Big[E\Big[|h_{N,u}-u_N|_{[0,T_N^n\wedge t_N]}+|h_{N,v}-v_N|_{[0,T_N^n\wedge t_N]}\\
&\qquad +\ |h_{N,l}-l_N|_{[0,T_N^n\wedge t_N]}\Big]\geq \bar{C}\delta_N^{1+2\rho}\Big]\\
&\leq P\Big[||h_{N,u}(0,\cdot)-u_N(0,\cdot)||_2^2+||h_{N,l}(0,\cdot)-l_N(0,\cdot)||_2^2\\
&\qquad +||h_{N,l}(0,\cdot)-l_N(0,\cdot)||_2^2+\alpha_N^{-1}\geq C\delta_N^{1+2\rho}\Big]\\
&<\epsilon(N),
\end{aligned}$$

where $\epsilon(N)$ when $N\to\infty$ (this is because of the assumptions on the constants α, δ, and the assumptions for time $t=0$). It follows that

$$\begin{aligned}
\lim_{N\to\infty} P\Big[&|h_{N,u}-u_N|_{[0,T_N^n\wedge t_N]}+|h_{N,v}-v_N|_{[0,T_N^n\wedge t_N]}\\
&+|h_{N,l}-l_N|_{[0,T_N^n\wedge t_N]}\geq \delta_N^{1+\rho}\Big]=0.
\end{aligned}$$

4.2. **Estimates for $|\mathbf{r_N}-\hat{\mathbf{r}}_\mathbf{N}|_{[\mathbf{0},\mathbf{T_N^n}\wedge\mathbf{t_N}]}$.** We now estimate the second term on the RHS of (40). Like before, we first look at $||r_N-\hat{r}_N||_2^2$. Since

$$\partial_t\langle u_N-\hat{u}_N,u_N-\hat{u}_N\rangle=2\langle u_N-\hat{u}_N,\partial_t(u_N-\hat{u}_N)\rangle$$

we get

$$\begin{aligned}
&||u_N(t,\cdot)-\hat{u}_N(t,\cdot)||_2^2=||u_N(0,\cdot)-\hat{u}_N(0,\cdot)||_2^2\\
&\quad+2\int_0^t\Big\langle u_N(\tau,\cdot)-\hat{u}_N(\tau,\cdot),\nabla\cdot\Big(\mu\nabla\big(u_N(\tau,\cdot)-\hat{u}_N(\tau,\cdot)\big)\Big)\Big\rangle\,d\tau\\
&\quad-2\int_0^t\Big\langle u_N(\tau,\cdot)-\hat{u}_N(\tau,\cdot),\nabla\cdot\Big(g_N(\tau,\cdot)u_N(\tau,\cdot)-\hat{g}_N(\tau,\cdot)\hat{u}_N(\tau,\cdot)\Big)\Big\rangle\,d\tau\\
&=||u_N(0,\cdot)-\hat{u}_N(0,\cdot)||_2^2-2\mu\int_0^t\big|\big|\nabla\big(u_N(\tau,\cdot)-\hat{u}_N(\tau,\cdot)\big)\big|\big|_2^2\,d\tau\\
&\quad-2\int_0^t\big\langle\nabla\big(u_N(\tau,\cdot)-\hat{u}_N(\tau,\cdot)\big),g_N(\tau,\cdot)\big(u_N(\tau,\cdot)-\hat{u}_N(\tau,\cdot)\big)\big\rangle\,d\tau\\
&\quad-2\int_0^t\big\langle\nabla\big(u_N(\tau,\cdot)-\hat{u}_N(\tau,\cdot)\big),\big(g_N(\tau,\cdot)-\hat{g}_N(\tau,\cdot)\big)\hat{u}_N(\tau,\cdot)\big\rangle\,d\tau.
\end{aligned}\tag{45}$$

Since g is bounded, the second integral on the RHS of (45) is bounded by

$$C\int_0^t\tilde{C}\,||u_N(\tau,\cdot)-\hat{u}_N(\tau,\cdot)||_2^2+\frac{1}{\tilde{C}}\,\big|\big|\nabla\big(u_N(\tau,\cdot)-\hat{u}_N(\tau,\cdot)\big)\big|\big|_2^2\,d\tau,$$

and an estimate for the last integral is

$$\begin{aligned}
C\int_0^t\Bigg[&\tilde{C}\left|\left|\frac{\hat{s}_{N,v}(\tau,\cdot)}{\hat{s}_{N,u}(\tau,\cdot)}-\frac{\hat{v}_N(\tau,\cdot)*\hat{W}_N}{\hat{u}_N(\tau,\cdot)*\hat{W}_N}\right|\right|_2^2+\tilde{C}\left|\left|\nabla\Big(\hat{s}_{N,l}(\tau,\cdot)-\hat{l}_N(\tau,\cdot)*\hat{W}_N\Big)\right|\right|_2^2\\
&+\frac{1}{\tilde{C}}\,\big|\big|\nabla\big(u_N(\tau,\cdot)-\hat{u}_N(\tau,\cdot)\big)\big|\big|_2^2\Bigg]d\tau.
\end{aligned}\tag{46}$$

From previous assumptions (46) is bounded by

$$C\int_0^t \Big[\tilde{C}\Big|\Big|\hat{s}_{N,u}(\tau,\cdot)-\hat{u}_N(\tau,\cdot)*\hat{W}_N\Big|\Big|_2^2+ \\ +\tilde{C}\Big|\Big|\nabla\Big(\hat{s}_{N,l}(\tau,\cdot)-\hat{l}_N(\tau,\cdot)*\hat{W}_N\Big)\Big|\Big|_2^2+\frac{1}{\tilde{C}}\big|\big|\nabla\big(u_N(\tau,\cdot)-\hat{u}_N(\tau,\cdot)\big)\big|\big|_2^2\Big]d\tau, \tag{47}$$

and one can estimate $||v_N(t,\cdot)-\hat{v}_N(t,\cdot)||_2^2$ and $||l_N(t,\cdot)-\hat{l}_N(t,\cdot)||_2^2$ the same way.

Also,

$$||l_N(t,\cdot)-\hat{l}_N(t,\cdot)||_2^2 \le \Big|\Big|l_N(0,\cdot)-\hat{l}_N(0,\cdot)\Big|\Big|_2^2 \\ -2\eta\int_0^t\Big|\Big|\nabla\big(l_N(\tau,\cdot)-\hat{l}_N(\tau,\cdot)\big)\Big|\Big|_2^2 d\tau + C\int_0^t||u_N(\tau,\cdot)-\hat{u}_N(\tau,\cdot)||_2^2\,d\tau \\ +C\int_0^t\Big|\Big|\hat{s}_{N,u}(\tau,\cdot)-\hat{u}_N(\tau,\cdot)*\hat{W}_N\Big|\Big|_2^2+\Big|\Big|\hat{s}_{N,l}(\tau,\cdot)-\hat{l}_N(\tau,\cdot)*\hat{W}_N\Big|\Big|_2^2 d\tau$$

leads to

$$\Big|l_N(t,\cdot)-\hat{l}_N(t,\cdot)\Big|_{[0,T_N^n\wedge t_N]} \le C\int_0^t||u_N(\tau,\cdot)-\hat{u}_N(\tau,\cdot)||_2^2\,d\tau \\ +C\int_0^t\Big|\Big|\hat{s}_{N,u}(\tau,\cdot)-\hat{u}_N(\tau,\cdot)*\hat{W}_N\Big|\Big|_2^2+\Big|\Big|\hat{s}_{N,l}(\tau,\cdot)-\hat{l}_N(\tau,\cdot)*\hat{W}_N\Big|\Big|_2^2 d\tau, \tag{48}$$

which has no term in $\Big|\Big|\nabla\Big(\hat{s}_{N,l}(\tau,\cdot)-\hat{l}_N(\tau,\cdot)*\hat{W}_N\Big)\Big|\Big|_2^2$. This is an important fact, because since

$$\Big|\Big|\nabla\Big(\hat{s}_{N,r}(\tau,\cdot)-\hat{r}_N(\tau,\cdot)*\hat{W}_N\Big)\Big|\Big|_2^2 \le \Big|\Big|\nabla\Big(h_{N,r}(\tau,\cdot)-\hat{r}_N(\tau,\cdot)\Big)\Big|\Big|_2^2 \\ \le \Big|\Big|\nabla\Big(h_{N,r}(\tau,\cdot)-r_N(\tau,\cdot)\Big)\Big|\Big|_2^2+\Big|\Big|\nabla\Big(r_N(\tau,\cdot)-\hat{r}_N(\tau,\cdot)\Big)\Big|\Big|_2^2,$$

we can use the above estimate (48) to bound the terms in $\Big|\Big|\nabla\Big(\hat{s}_{N,l}(\tau,\cdot)-\hat{l}_N(\tau,\cdot)*\hat{W}_N\Big)\Big|\Big|_2^2$ coming from the estimates for $||u_N(t,\cdot)-\hat{u}_N(t,\cdot)||_2^2$ and $||v_N(t,\cdot)-\hat{v}_N(t,\cdot)||_2^2$. Hence,

for $\tilde{T} \leq T$, and assuming $\tilde{C} > 1$, we have

$$\begin{aligned}
\sum_{r=u,v,l} \Bigg[& \sup_{t\leq \tilde{T}\wedge T_N^n \wedge t_N} ||r_N(t,\cdot) - \hat{r}_N(t,\cdot)||_2^2 \\
& + \int_0^{\tilde{T}\wedge T_N^n\wedge t_N} \Big|\Big|\nabla\Big(r_N(\tau,\cdot) - \hat{r}_N(\tau,\cdot)\Big)\Big|\Big|_2^2 d\tau \Bigg] \leq C\tilde{C} \sum_{r=u,v,l} ||r_N(0,\cdot) - \hat{r}_N(0,\cdot)||_2^2 \\
& + C\int_0^t \tilde{C}\, ||u_N(\tau,\cdot) - \hat{u}_N(\tau,\cdot)||_2^2 + \frac{1}{\tilde{C}} \Big|\Big|\nabla\big(u_N(\tau,\cdot) - \hat{u}_N(\tau,\cdot)\big)\Big|\Big|_2^2 d\tau \\
& + \frac{1}{\tilde{C}} \sum_{r=u,v,l} \int_0^{\tilde{T}\wedge T_N^n\wedge t_N} \Big|\Big|\nabla\Big(r_N(\tau,\cdot) - \hat{r}_N(\tau,\cdot)\Big)\Big|\Big|_2^2 d\tau \\
& + \tilde{C} \sum_{r=u,v,l} \int_0^{\tilde{T}\wedge T_N^n\wedge t_N} \sup_{\sigma\leq\tau} ||r_N(\sigma,\cdot) - \hat{r}_N(\sigma,\cdot)||_2^2 \, d\tau \\
& + \tilde{C}\tilde{T} \sum_{r=u,v,l} \sup_{t\leq \tilde{T}\wedge T_N^n\wedge t_N} ||s_{N,r}(t,\cdot) - r_N(t,\cdot)||_2^2 \\
& + \tilde{C} \int_0^{\tilde{T}\wedge T_N^n\wedge t_N} \Big|\Big|\nabla\Big(s_{N,l}(\tau,\cdot) - l_N(\tau,\cdot)\Big)\Big|\Big|_2^2 d\tau.
\end{aligned}$$

Thus for for $\tilde{C}$ large, one gets using Gronwall's inequality,

$$\begin{aligned}
& P\left[\sum_{r=u,v,l} |r_N(t,\cdot) - \hat{r}_N(t,\cdot)|_{[0,T_N^n\wedge t_N]} > \frac{\delta_N}{2}\right] \\
& \leq P\Bigg[\tilde{C}e^{\tilde{C}T_N^n}\Bigg(\sum_{r=u,v,l} ||r_N(0,\cdot) - \hat{r}_N(0,\cdot)||_2^2 + \sum_{r=u,v,l} \sup_{t\leq T_N^n\wedge t_N} ||s_{N,r}(t,\cdot) - r_N(t,\cdot)||_2^2 \\
& \qquad + \int_0^{\tilde{T}\wedge T_N^n\wedge t_N} \Big|\Big|\nabla\Big(s_{N,l}(\tau,\cdot) - l_N(\tau,\cdot)\Big)\Big|\Big|_2^2 d\tau\Bigg) > \frac{\delta_N}{2}\Bigg] \\
& \leq P\Bigg[\tilde{C}e^{\tilde{C}T_N^n}\Bigg(\sum_{r=u,v,l} ||r_N(0,\cdot) - \hat{r}_N(0,\cdot)||_2^2 \\
& \qquad + \sum_{r=u,v,l} |s_{N,r}(t,\cdot) - r_N(t,\cdot)|_{[0,T_N^n\wedge t_N]}\Bigg) > \frac{\delta_N}{2}\Bigg].
\end{aligned}$$

From the result in 4.1 and the assumptions for $t = 0$, this quantity goes to zero as $N \to \infty$. Thus the second term of (40) is valid and (32) follows.

5. **Conclusion.** In this paper we have derived a hierarchy of models for describing the motion of phototaxis. The novelty of our approach was in assuming that the motion of the colony of bacteria strongly depends on group dynamics, rather on decisions made by individual bacteria. The postulated group dynamics (whose existence is evident in the experimental data) was incorporated into the models through the excitation property.

The phototaxis system (24) we obtained, resembles the known chemotaxis system The main differences between both systems are related to both the existence of an internal property, and the restrictions imposed on the parameter functions. For

example, in the phototaxis system it is assumed that the velocity is bounded. This is not the case with the chemotaxis system.

While the analysis presented in this paper closely follows the methods of [14, 18] the additional excitation property, who really is a property of every individual bacteria, adds another layer of difficulty to the analysis. From an analytical point of view, the phototaxis system does pose several difficulties as there is a system-wide dependence on v/u and g depends on ∇l in a nonlinear manner.

The method used in this paper works only for a diffusing surface memory effect. The details of the analysis as presented here do not allow sensitivity function g to depend on any derivative besides ∇l. It would be interesting to study the effects of adding such terms into the phototaxis system, i.e., a system of the form

$$\begin{cases} \partial_t u = \mu\Delta u - \nabla \cdot \big(g(u, v, l, \nabla u, \nabla l)u\big), \\ \partial_t v = \mu\Delta v - \nabla \cdot \big(g(u, v, l, \nabla u, \nabla l)v\big) + \beta(u, v)u - \gamma(u, v)v, \\ \partial_t l = \lambda(u, l)u. \end{cases}$$

Such a system will allow, e.g., to directly consider a motion of the bacteria that tends towards areas of a large density of bacteria.

An extensive simulation study of the stochastic model to determine the dependency of the results on the values of the different parameters and on the choice of the response functions is currently under way and will be separately reported in [5].

Finally, it will be very interesting to see if the phototaxis system (24) does support the formation of some of the structures that are observed experimentally, such as the fingers and the pinching. This may depend on the choice of parameter functions, such as g, β, and γ. Such a study is beyond the scope of this introductory paper and is left to a future work.

Acknowledgments. The work of D. Levy was supported in part by the NSF under Career Grant DMS-0133511. We would like to thank Devaki Bhaya and Matthew Burriesci for generating the images and movies and for their guidance.

REFERENCES

[1] J.P. Armitage, *Bacterial tactic responses*, Adv. Microb Physiol., **41** (1999), 229–289.
[2] D. Bhaya, *Light matters: Phototaxis and signal transduction in unicellular cyanobacteria*, Mol. Microbiol., **53** (2004), 745–754.
[3] D. Bhaya, N. R. Bianco, D. Bryant, and A. R. Grossman, *Type IV pilus biogenesis and motility in the cyanobacterium Synechocystis sp. PCC6803*, Mol. Microbiol., **37** (2000), 941–951,
[4] D. Bhaya, D. Levy and T. Requeijo, *Group Dynamics of Phototaxis: Interacting Stochastic Many-Particle Systems and their Continuum Limits* To appear in Proceedings of HYP 2006, Lyon.
[5] D. Levy and T. Requeijo, *Stochastic Models for Phototaxis: a Simulation Study*, in preparation.
[6] D. Bhaya, A. Takahashi, and A. R. Grossman, *Light regulation of TypeIV pilus-dependent motility by chemosensor-like elements in Synechocystis PCC 6803*, Proc. Natl. Acad. Sci. U.S.A., **98** (2001), 7540–7545.
[7] M. Burriesci and D. Bhaya, *Tracking the motility of single cells and groups of Synechocystis sp. strain PCC6803 during phototaxis*, in preparation.
[8] B. Chopard, P. Luthi, and A. Masselot, *Cellular automata and lattice boltzmann techniques: An approach to model and simulate complex systems*, citeseer.ist.psu.edu/chopard98cellular.html.
[9] B. Davis, *Reinforced Random Walks*, Probability Theory Related Fields, **84** (1990), 203–229.
[10] A. Friedman, *Partial Differential Equations of Parabolic Type*, Robert E. Krieger Publishing Company, Malabar, FL, 1983.

[11] T. Hillen, K. Painter, and C. Schmeiset, *Global Existence for Chemotaxis with Finite Sampling Radius*, Disc. Cont. Dyn. Sys. B, **7** (2007), 125–144.
[12] E.F. Keller and L.A. Segel, *Traveling band of chemotactic bacteria: a theoretical analysis*, J. Theor Biology, **30** (1971), 235–248.
[13] L.L. McCarter, *Regulation of flagella*, Curr Opin Microbiol., **9** (2006), 180–186.
[14] K. Oelschläger, *On the derivation of reaction-diffusion equations as limit dynamics of systems of moderately interacting stochastic many-particle processes*, Probability Theory Related Fields, **82** (1989), 565–586.
[15] B. Øksendal, *Stochastic Differential Equations*, Springer, Fifth Edition, 2002.
[16] C.S. Patlack, *Random walk with persistence and external bias*, Bull. Math. Biophys, **15** (1953), 311–338.
[17] A. Stevens, *A stochastic cellular automaton modeling gliding and aggregation of myxobacteria*, SIAM Journal of Applied Mathematics, **61** (2000), 172–182.
[18] A. Stevens, *The derivation of chemotaxis equations as limit dynamics of moderately interacting stochastic many-particle systems*, SIAM Journal of Applied Mathematics, **61** (2000), 183–212.
[19] S. Childress and M. Levandowsky and E. Spiegel, *Pattern Formation in a Suspension of Swimming Microorganisms: Equations and Stability Theory* Journal of Fluid Mechanics, **63** (1975), 591
[20] S. Childress and M. Levandowsky and E. Spiegel and S. Hunter, *A Mathematical Model of Pattern Formation by Swimming Microorganisms*, J. Protozool. **22** (1975), 296
[21] A. Maree and A. Panfilov and P. Hogeweg, *Phototaxis during the slug stage of Dictyostelium discoideum: a model study* Proc. R. Soc. Lond. **B** (1999) 266, 1351-1360
[22] T. Nutsch and W. Marwan and D. Oesterhelt and E. Gilles *Signal Processing and Flagellar Motor Switching During Phototaxis of Halobacterium salinarum* Genome Res. **13** (2003), 2406-2412

Received xxx xx, 200x; revised xxx 200x.

E-mail address: dlevy@math.umd.edu; requeijo@math.stanford.edu